HHS Public Access

Author manuscript

Biochim Biophys Acta Mol Basis Dis. Author manuscript; available in PMC 2023 January 01.

Published in final edited form as:

Biochim Biophys Acta Mol Basis Dis. 2022 January 01; 1868(1): 166288. doi:10.1016/j.bbadis.2021.166288.

GPR65 (TDAG8) inhibits intestinal inflammation and colitis-associated colorectal cancer development in experimental mouse models

Mona A. Marie[a,*], **Edward J. Sanderlin**[a,*], **Swati Satturwar**[b], **Heng Hong**[b,f], **Kvin Lertpiriyapong**[d,e], **Deepak Donthi**[b], **Li V. Yang**[a,c,#]

[a]Department of Internal Medicine, Brody School of Medicine, East Carolina University, USA

[b]Department of Pathology, Brody School of Medicine, East Carolina University, USA

[c]Department of Anatomy and Cell Biology, Brody School of Medicine, East Carolina University, USA

[d]Department of Comparative Medicine, Brody School of Medicine, East Carolina University, USA

[e]Center for Comparative Medicine and Pathology, Memorial Sloan Kettering Cancer Center, USA

[f]Department of Pathology, Wake Forest University, USA

Abstract

GPR65 (TDAG8) is a proton-sensing G protein-coupled receptor predominantly expressed in immune cells. Genome-wide association studies (GWAS) have identified GPR65 gene polymorphisms as an emerging risk factor for the development of inflammatory bowel disease (IBD). Patients with IBD have an elevated risk of developing colorectal cancer when compared to the general population. To study the role of GPR65 in intestinal inflammation and colitis-associated colorectal cancer (CAC), colitis and CAC were induced in GPR65 knockout (KO) and wild-type (WT) mice using dextran sulfate sodium (DSS) and azoxymethane (AOM)/DSS, respectively. Disease severity parameters such as fecal score, colon shortening, histopathology, and mesenteric lymph node enlargement were aggravated in GPR65 KO mice compared to WT mice treated with DSS. Elevated leukocyte infiltration and fibrosis were observed in the

[#]Corresponding author: Li V. Yang, Ph.D., Department of Internal Medicine, East Carolina University, Greenville, NC 27834, USA; Phone: +1-252-744-3419; Fax: +1-252-744-3418; yangl@ecu.edu.

[*]Contributed equally

Author Contributions

M.A.M., E.J.S., K.L., and L.V.Y. designed experiments. M.A.M. and E.J.S. performed experiments. M.A.M., E.J.S., and L.V.Y. analyzed the data. S.S., H.H., and D.D. performed histopathological analyses. L.V.Y. supervised this study. M.A.M., E.J.S., and L.V.Y. wrote the manuscript. All authors edited and revised the manuscript.

Declaration of interests

The authors declare that they have no known competing financial interests or personal relationships that could have appeared to influence the work reported in this paper.

Conflict of Interest

None.

inflamed colon of GPR65 KO when compared to WT mice which may represent a cellular mechanism for the observed exacerbation of intestinal inflammation. In line with high expression of GPR65 in infiltrated leukocytes, GPR65 gene expression was increased in inflamed intestinal tissue samples of IBD patients compared to normal intestinal tissues. Moreover, colitis-associated colorectal cancer development was higher in GPR65 KO mice than WT mice when treated with AOM/DSS. Altogether, our data demonstrate that GPR65 suppresses intestinal inflammation and colitis-associated tumor development in murine colitis and CAC models, suggesting potentiation of GPR65 with agonists may have an anti-inflammatory therapeutic effect in IBD and reduce the risk of developing colitis-associated colorectal cancer.

Keywords

GPR65 (TDAG8); Inflammatory bowel disease (IBD); Colorectal cancer

1. Introduction

Genome-wide association studies (GWAS) have discovered numerous genetic risk loci for chronic inflammatory diseases. Large-scale GWAS studies have identified GPR65 (also known as T-cell death-associated gene 8, TDAG8) as a susceptibility candidate gene for several human chronic inflammatory diseases such as multiple sclerosis, asthma, spondylarthritis, and inflammatory bowel disease (IBD) [1–4]. The GPR65 gene locus is also associated with IBD susceptibility in mice [5]. GPR65-deficient mice are more susceptible to bacteria-induced colitis and an IBD-associated GPR65 genetic variant (I231L) confers reduced GPR65 signaling activity as well as impaired lysosomal function [6]. Moreover, GPR65 deficiency increases intestinal inflammation in murine IBD models [7]. These data suggest GPR65 activation could inhibit inflammation in certain diseases such as IBD.

GPR65 (TDAG8) was initially identified as a gene upregulated during T cell activation and apoptosis [8, 9]. GPR65 is highly expressed in leukocytes and leukocyte-rich tissues such as the spleen, lymph nodes, and thymus. Biochemically, GPR65 can be activated by acidic extracellular pH through the protonation of several histidine residues on the receptor extracellular domains and transduce downstream signals through the G_s/cAMP and $G_{12}/_{13}$/Rho GTPase pathways [10–18].

It has long been observed that the inflammatory loci can be more acidic than non-inflamed tissues and that acidic pH can alter the function of inflammatory cells, vascular cells, and other stromal cells [13, 17, 19–26]. The ways in which immune cells sense extracellular pH within inflamed microenvironments and subsequently alter their phenotypes have only recently been investigated. The role of GPR65 activation by inflammation-associated acidosis has been investigated both *in vitro* and *in vivo*. Functionally, both pro- and anti-inflammatory effects of GPR65 have been described [3, 6, 10, 12, 16, 27–31]. GPR65 has been reported to impede proinflammatory profiles of primary murine macrophages, T cells, and microglia [10, 12, 29, 32]. Investigation of GPR65 in animal models of acute lung

injury, arthritis, myocardial infarction, and colitis have indicated GPR65 functions to inhibit inflammation in a variety of inflammatory diseases [6, 16, 30, 31].

IBD is a broad term covering both Crohn's disease (CrD) and ulcerative colitis (UC) [33]. IBD is characterized by recurrent, aberrant inflammation within the intestinal tissue. These two disease forms are distinct yet have overlapping clinical and histopathological features. The exact etiology is unknown; however, a complex interaction between immunologic, environmental, and genetic constituents is believed to contribute to the disease onset and progression. Chronic inflammation associated with IBD is a key player in modulating the intestinal microenvironment leading to colorectal cancer development [34]. As such, IBD patients have a higher risk of developing colorectal cancer than the general population [35].

As aberrant GPR65 function is associated with IBD in patients [4, 6], we sought to utilize the dextran sulfate sodium (DSS)-induced colitis mouse model and the azoxymethane (AOM)/DSS-induced colitis-associated colorectal cancer (CAC) mouse model to evaluate the role of GPR65 in intestinal inflammation and CAC development. Our results demonstrate that GPR65 is protective against colonic inflammation, IBD associated complications, and CAC development.

2. Materials and Methods

2.1. Dextran sulfate sodium (DSS)-induced colitis mouse model

Male and female wild-type (WT) and GPR65 knockout (KO) mice at 9 weeks old were used in the experiments. GPR65 KO mice were generated as previously described [36] and backcrossed 9 generations into the C57BL/6J background. Animals were maintained under specific pathogen-free conditions and were free from exogenous murine viruses, *Helicobacter*, ectoparasites, and endoparasites. Mice were housed in an AAALAC-accredited facility under environmental conditions of a 12:12 light/dark cycle, temperature at 22 ± 1 °C and relative humidity range of 30–70%. Mice were group housed in microisolator cages and provided with autoclaved tap water and pelleted diet (ProLab 2000, St. Louis, MO) *ad libitum*. Colitis was induced using 3% (w/v) colitis grade dextran sulfate sodium (DSS) with molecular weight 36,000–50,000 Da (Lot# Q1408, MP Biomedical, Solon, OH) within the drinking water of mice [25, 37]. The 3% DSS solution or water was provided to mice *ad libitum*. In order to recapitulate human disease relapse and remission, mice were given 3% DSS for 4 cycles. Each cycle constituted 5 days of 3% DSS followed by 2 days of water. Following the fourth cycle, water was switched back to 3% DSS for 2 final days. Mouse body weight and clinical phenotype scores were measured each day. All animal experiments were performed according to the randomized block experimental design [25]. The mouse experiments were approved by the Institutional Animal Care and Use Committee of East Carolina University in accordance with the *Guide for the Care and Use of Laboratory Animals* (The National Academies Press).

2.2. Azoxymethane (AOM) and dextran sulfate sodium (DSS)-induced colitis associated colorectal cancer mouse model

Experiments were performed using 9 to 12 weeks old male and female WT and GPR65 KO mice. Mice were backcrossed 9–10 generations into the C57BL/6J background. Colitis-associated colorectal cancer was induced in mice using a single *i.p.* injection (10mg/kg) of azoxymethane (AOM, product# A5486, Sigma-Aldrich, Saint Louis, MO) followed by 4% (w/v) DSS (Lot# Q5229 and S0948, MP Biomedical, Solon, OH) in drinking water. The treatment schedule was adapted from previously described [38] in which mice were given 4% DSS in water for 3 cycles. Each cycle constituted 5 days of 4% DSS followed by 16 days of water. Following the third cycle, mice were given water for the remaining period to the endpoint on the 13–14th week. Mouse body weight was measured each day for the first 14 days of each cycle. All animal experiments were performed according to the randomized block experimental design [25].

2.3. Clinical phenotype scoring

Colitis severity was evaluated using the clinical parameters of body weight loss and fecal score [25]. Disease activity index represented by body weight loss percentage, fecal score, colon shortening, lymph node expansion and spleen weight was measured to assess inflammation in WT and GPR65 mice treated with DSS or AOM/DSS. Feces was collected from mice and assessed for presence of blood and consistency. Fecal scoring system consisted of the following: 0= normal, dry, firm pellet; 1= formed soft pellet with negative hemoccult test, 2= formed soft pellet with positive hemoccult test; 3= formed soft pellet with visual blood; 4= liquid diarrhea with visual blood; 5= no colonic fecal content and bloody mucus upon necropsy [25]. Presence of micro blood content was measured using the Hemoccult Single Slides screening test (Beckman Coulter, Brea, CA).

2.4. Tissue collection, evaluation, and processing

Upon the study endpoint, mice were euthanized followed by necropsy. Colon length was measured from the ileocecal junction to anus. Colon was then removed from cecum and the colon lumen was cleared of fecal content by washing with phosphate buffer saline (PBS) and then opened along the anti-mesenteric border. The colon tissue was then fixed with 10% buffered formalin and cut evenly into distal, mid, and proximal sections for histologic evaluation. The mesenteric lymph node and tumor polyps were collected for histological analysis and the volume was assessed with a caliper using the formula (length × width^2) $\pi/6$ [25]. Lymph nodes and colon tissues were then fixed with 10% formalin for histological analysis. Mouse spleens were also collected and weighed.

2.5. Histopathological analysis

Five μm sections of distal, middle, and proximal colon tissue segments were obtained from WT and GPR65 KO mice treated with DSS or AOM/DSS and stained with hematoxylin and eosin (H&E) for histological analysis. Sample identification was concealed during histopathological analysis for unbiased evaluation. Board certified medical pathologists (S.S., D.D. & H.H.) evaluated colitis histopathological features including inflammation, crypt damage, edema, architectural distortion, and leukocyte infiltration in a blinded manner

as previously described [25, 39, 40]. Each parameter was scored and multiplied by a factor corresponding to total disease involvement. Additional scoring criteria of colonic fibrosis were evaluated as previously described [41]. Briefly, colon segments of WT and GPR65 KO mice treated with DSS or AOM/DSS were stained with picrosirius red and Masson's Trichrome for fibrosis analysis and graded in a blinded manner for pathological fibrosis. Severity of fibrosis was included as one of the parameters of the histopathological score.

2.6. Immunohistochemistry

Colon tissues and mesenteric lymph nodes were embedded in paraffin and serial five μm sections were evaluated for immunohistochemical analysis as previously described [25]. Briefly, antigen retrieval was performed of colon and mesenteric lymph node sections followed by endogenous peroxidase blocking. Tissue segments were blocked with normal serum and stained with anti-Green Florescence Protein (GFP) (Abcam, ab6673, Cambridge, MA), anti-F4/80 (Invitrogen, SP115, Waltham, MA), anti-CD3 (Sigma, St. Louis, MO), anti-CD45 (Abcam, ab25386, Cambridge, MA), and anti-αSMA (Sigma, St. Louis, MO) primary antibodies. The IHC detection system HRP-DAB Cell and Tissue staining kit (R&D Systems, Minneapolis, MN) or Superpicture 3rd Gen IHC Detection system (Invitrogen, Waltham, MA) were used. Following addition of secondary antibody, DAB (3,3' –diaminobenzidine) incubation was performed for HRP detection. Pictures were taken using the Zeiss Axio Imager M2 microscope.

2.7. Isolated lymphoid follicle quantification

Serial tissue sections of the colons were stained with H&E. Distal, middle, and proximal colon segments were scanned using a light microscope with 4× and 10× objectives in a blinded manner and isolated lymphoid follicles (ILFs) were counted. Colon segments were measured using a caliper for length in centimeters. Data are presented as ILFs/centimeter (cm).

2.8. Leukocyte quantification

Distal colon tissue segments were randomly selected from WT and GPR65 mice treated with DSS or AOM/DSS. Slides from WT and GPR65 KO DSS-treated mouse colons were stained for macrophage F4/80 and T cell CD3 markers. Slides from AOM/DSS-treated WT and GPR65 KO mouse colons were stained for the pan leukocyte marker CD45. Picture were taken (n=8–12) sequentially starting from the anus of the distal segment of the colon at 400× magnification. Positively stained immune cells were manually quantified using ImageJ software per high power field of view (FOV) and then averaged per mouse. H&E slides for WT and GPR65 KO DSS mice were used to quantify neutrophils based on the characteristic polymorphonuclear morphology. The sample identification was concealed during cell counting and scoring.

2.9. Real-time RT-PCR

Real-time RT-PCR was performed as previously described using the TaqMan pre-designed primer-probe sets for β-actin (Hs01060665_g1), GPR65 (Hs00269247_s1), TNFα (Hs00174128_m1), and IFNγ (Hs00989291_m1) [25]. Crohn's and colitis cDNA array

were purchased from Origene Technologies (Catalog #CCRT102, Rockville, MD) to assess GPR65 gene expression in human inflammatory bowel disease lesions compared to non-inflamed intestinal tissues. Intestinal inflammation, including leukocyte infiltration, was verified by accompanied histopathological analyses of the samples provided by the vendor. All sample information can be found in a previous report [25].

2.10. Statistical analysis

All statistical analysis was performed using the GraphPad Prism software. The unpaired t-test and the Mann-Whitney test were used to compare differences between two groups (WT vs. GPR65 KO). Correlation of gene expression was determined by the linear regression analysis. $P < 0.05$ is considered statistically significant.

3. Results

3.1. Genetic deletion of GPR65 exacerbates intestinal inflammation and fibrosis in the chronic DSS-induced colitis mouse model

To characterize the role of GPR65 in colitis, we utilized the DSS-induced mouse model for the induction of chronic intestinal inflammation [37]. During the experiment, clinical parameters such as body weight loss and fecal blood and diarrhea score were assessed. Interestingly, control GPR65 KO mice gained more weight than control WT mice during the experiment. Similar trend was observed in both male and female mice (Supplementary Fig. 1). To uncover the effects of DSS more precisely, WT-DSS and GPR65 KO-DSS mouse body weight loss was normalized to the control mice. No significant difference in the normalized body weight loss was observed between WT-DSS and GPR65 KO-DSS mice during the first cycle; however, GPR65 KO-DSS mice trended more body weight loss with most significant weight loss occurring at the end of second cycle and third cycle compared to WT-DSS mice (Fig. 1A). Fecal scores also indicated heightened severity of GPR65 KO-DSS mice compared to WT-DSS mice (Fig. 1B). Both WT-DSS and GPR65 KO-DSS mice reached an average fecal score of 3 by the end of the first cycle; however, GPR65 KO-DSS mice maintained a more severe score during the second cycle and the third cycle compared to WT-DSS mice. Interestingly, during the fourth cycle the GPR65 KO-DSS mice partially recovered compared to WT-DSS, which could be due in part to elevated body weight gain in GPR65 KO control mice when compared to WT (Fig. 1A, Supplementary Fig. 1). Upon the terminal point of the experiment, macroscopic disease indicators were evaluated such as mesenteric lymph node expansion and colon length shortening. Expansion of mesenteric lymph nodes (MLN) is a common parameter for colonic inflammation in the DSS-induced colitis model. Untreated control mice had MLN volumes approximately 5–6 mm^3 for WT and GPR65 KO mice. MLN volume was significantly increased in DSS-treated mice as WT-DSS mice had an average volume of ~20 mm^3. Interestingly, GPR65 KO-DSS MLN expansion (~40 mm^3) was almost 2-fold higher than WT-DSS (Fig. 1C), indicating the inflammation of GPR65 KO-DSS was more severe than WT-DSS. Finally, colon length was measured to assess the degree of shortening, which corresponds to heightened DSS-induced inflammation. WT-DSS mice had ~7% shortening compared to WT-untreated mice. GPR65 KO-DSS mice, however, had ~13% colon shortening when compared to KO-untreated mice. No statistically significant differences existed between WT-DSS and GPR65 KO-DSS mice

which could be due to slightly longer colon lengths observed in GPR65 KO control mice when compared to WT mice (Fig. 1D).

To further assess the role of GPR65 in intestinal inflammation, histopathological analysis was performed to quantify the degree of histological features of colitis between WT and GPR65 KO mice. Distal, middle, and proximal segments of the colon were examined for common histopathological features of colitis, such as leukocyte infiltration, inflammation, edema, crypt damage, architectural distortion, and fibrosis. Untreated control mice had no colitis histopathological features. The GPR65 KO-DSS mice were more severe than WT-DSS mice in terms of total histopathology and fibrosis in the distal colon (Fig. 2). The highest histopathology was observed in the distal colon and is consistent with previous studies showing DSS model affects distal colon most severely [40, 41].

Isolated lymphoid follicles (ILFs) are tertiary lymphoid tissues which can be induced within inflamed murine intestinal tissues. We have previously reported that ILFs are increased in intestinal tissues of mice in the DSS-induced acute colitis model when compared to untreated control mice [25]. Here we demonstrate that ILF numbers are increased in areas of heightened colonic inflammation and are further increased in mice deficient of GPR65 (Supplementary Fig. 2). ILFs were less prevalent in proximal segment when compared to middle and distal inflamed colon segments in both WT-DSS and GPR65 KO-DSS mice (Supplementary Fig. 2E). GPR65 KO-DSS mice had increased ILFs/centimeter within each colon segment and subsequently full-length colon when compared to WT-DSS (Supplementary Fig. 2E–F). These data suggest GPR65 reduces inflammation-associated ILF development.

Fibrosis is another pathological feature of IBD and can lead to life-threatening complications [42]. Colon segments were stained with picrosirius red and Masson's trichrome for the assessment of colonic fibrosis after chronic intestinal inflammation (Fig. 2E–H and Supplementary Fig. 3). The greatest degree of fibrosis was found in DSS distal colons with a gradual decrease in fibrosis towards proximal colon (Fig. 2J). We observed an increase in fibrosis within distal colon of GPR65 KO-DSS mice compared to WT-DSS mice. Severely fibrotic areas of the colon were characterized by increased collagen deposition within the lamina propria, muscularis mucosa, muscularis externa, and serosa when compared to control tissues (Fig. 2E–H, Supplementary Fig. 3).

To further investigate why GPR65 KO-DSS mice had heightened fibrosis compared to WT-DSS mice, we examined myofibroblasts within the inflamed and fibrotic distal colon mucosa. Myofibroblasts are one of several cellular constituents which can contribute to intestinal fibrosis [42]. Normal intestinal myofibroblasts exist subjacent to the epithelium and regulate tissue repair, fibrosis, glandular secretion, and mucosal regeneration. α-SMA$^+$ myofibroblasts within distal colon segments were evaluated (Fig. 3). There was a discernable increase in sub-epithelial mucosal myofibroblasts between WT-control and WT-DSS mice and a further increase in GPR65 KO-DSS mice (Fig. 3). Very few myofibroblasts were observed within the submucosa. Increased myofibroblasts could be detected within ulcerated areas of the colon when compared to non-ulcerated colon areas. Furthermore,

during epithelial cell loss within ulcerated regions of the colon, myofibroblasts could be observed interspersing within disrupted epithelium for mucosal repair (Fig. 3E–F).

3.2. Leukocyte infiltration is increased in the colon of DSS-treated GPR65-null mice

To further characterize colonic inflammation differences between WT-DSS and GPR65 KO-DSS mice, we examined the populations of inflammatory cell infiltrates. The numbers of neutrophils, macrophages, and T cells within the distal colon were assessed. In the untreated control mouse distal colons, very few neutrophils (~3 cells/field), T cells (~6 cells/field) and some macrophages (~30 cells/field) were observed in the mucosal layer (Supplementary Fig. 4). No significant difference was observed between control WT and GPR65 KO mice. There was an increase in polymorphonuclear neutrophil, F4/80^{+} macrophage, and CD3^{+} T cell numbers in the distal colons between untreated and DSS-treated mice. We observed a 20–30% increase in leukocyte infiltrates within GPR65 KO-DSS tissues when compared to WT-DSS distal colon tissues (Fig. 4).

3.3. GPR65 gene expression in the mouse colon is predominantly detected in interstitial leukocytes

GPR65 has been reported to be highly expressed in immune cells and leukocyte rich tissues such as the spleen, lymph nodes, and thymus [8, 9, 36]. Increased GPR65 expression can also be observed in tissues with higher baseline levels of resident leukocytes such as the lung and intestinal tissues. GPR65 localization has not yet been investigated within the colon and mesenteric lymph nodes (MLN), most likely due to the lack of a reliable antibody. To investigate GPR65 expression within the colon and MLN, we performed immunohistochemistry for green fluorescence protein (GFP) which functions as a surrogate marker for GPR65 gene expression within GPR65 KO mice [36]. GPR65 KO mice were generated by replacing the GPR65 coding region with a promoterless internal ribosomal entry site (IRES)-GFP cassette [36]. Therefore, GFP expression is under the control of the endogenous GPR65 promoter. GFP was detected in interstitial leukocytes within colon mucosa, transverse folds, and intestinal isolated lymphoid follicles (Fig. 5). Additionally, high GFP expression could be observed in MLN of untreated GPR65 KO mice. Based on cellular morphology and localization, GFP expression within these colon leukocytes appears to be predominately macrophages, neutrophils, and lymphocytes. Within the MLN, high GFP expression was detected in histocytes and lymphocytes within the sinus regions, B cell follicles/germinal centers, and paracortical/interfollicular T cell zone. GFP expression was also assessed in DSS-treated GPR65 KO mouse colon and MLN. A discernable increase of GFP positive leukocytes could be detected within the inflamed colon mucosa and transverse folds when compared to non-inflamed colon tissues. GFP could also be highly detected in ILFs and MLNs as observed in untreated mice. GFP expression is negative in both untreated and DSS-treated GPR65 KO mouse epithelial cells and mesenchymal cells such as fibroblasts and smooth muscle cells. Additionally, endothelial cells are negative for GFP expression. There was also no GFP signal detected in any WT mouse tissues (Supplementary Fig. 5).

3.4. GPR65 gene expression is increased in inflamed intestinal tissues of IBD patients

GPR65 gene expression was assessed in intestinal tissues from patients with ulcerative colitis (UC) and Crohn's disease (CrD) in comparison to normal intestinal tissues. A cDNA array including 7 non-inflamed intestinal tissue samples, 14 CrD tissue samples, and 26 UC tissue samples was utilized. Intestinal inflammation, such as leukocyte infiltration, was verified by histopathological analyses of the CrD and UC samples. We observed a 3.2-fold increase of GPR65 gene expression in UC samples and a 5.2-fold increase in CrD samples compared to normal intestinal samples (Fig. 6A). We next assessed inflammatory gene expression and observed elevated levels of TNFα and IFNγ mRNA in UC and CrD samples when compared to control tissues (Fig. 6A). Interestingly, elevated GPR65 mRNA levels were positively correlated with increases in TNFα and IFNγ gene expression in IBD intestinal tissues (Fig. 6B). The increase of GPR65 gene expression and the positive correlation with inflammatory gene expression could be partly due to infiltrated leukocytes which highly express GPR65 in inflamed intestinal tissues (Figs. 2, 4, and 5).

3.5. Genetic deletion of GPR65 increases intestinal tumorigenesis in the AOM/DSS mouse colitis-associated colorectal cancer (CAC) model

Chronic intestinal inflammation is associated with a higher risk of developing colorectal cancer in IBD patients [43–45]. We assessed the role of GPR65 in the development of colitis associated colorectal cancer (CAC) using the AOM/DSS mouse model. WT and GPR65 KO mice were injected with azoxymethane (AOM) followed by DSS administration for the development of inflammation-associated colorectal cancer. Tumor burden was represented by both polyp/tumor incidence and tumor volume in the mouse colon. A significant increase of ~2-fold in polyp/tumor numbers were observed in GPR65 KO-AOM/DSS when compared to WT-AOM/DSS mouse colon tissues. The majority of tumor polyps were observed in the distal colon with decreasing tumor numbers in middle and proximal colon segments. Similarly, the total volume of tumor polyps in GPR65 KO-AOM/DSS mice were elevated by ~2-fold when compared to WT-AOM/DSS mice (average total volume of ~ 66 mm^3/colon vs. 31 mm^3/colon, respectively) (Fig. 7A–D). Histological analyses of the colon sections harboring tumor polyps revealed colon dysplasia and adenocarcinoma were induced in both WT-AOM/DSS and GPR65 KO-AOM/DSS mice (Fig. 7E–H). While the total number of lesions observed was higher in GPR65 KO-AOM/DSS mouse colons, the relative distribution of colon dysplasia and adenocarcinoma was similar between WT- and GPR65 KO-AOM/DSS mice.

3.6. Aggravated intestinal inflammation is associated with increased tumorigenesis in the CAC mouse model

Inflammation is a driving force for tumorigenesis in the AOM/DSS colitis-associated colorectal cancer model [46, 47]. Consistent with the phenotype observed in the DSS-induced colitis mouse model (Figs. 1–4), colon shortening, body weight loss, spleen enlargement, and mesenteric lymph node expansion were more severe in the GPR65 KO-AOM/DSS mice than the WT-AOM/DSS mice (Fig. 8A–B and Supplementary Fig. 6). Histological analyses revealed higher levels of fibrosis and myofibroblast expansion in the colon of GPR65 KO-AOM/DSS mice when compared to WT-AOM/DSS mice (Fig. 8C–

E). To assess leukocyte infiltration throughout the colon, tissue sections were stained for CD45, a pan-leukocyte marker. A significant increase of leukocyte infiltration in the distal, middle, and proximal colon of GPR65 KO-AOM/DSS mice was observed when compared to WT-AOM/DSS mice (Fig. 9). Altogether, these results suggest that the aggravated intestinal inflammation is associated with the increased polyp and tumor formation in the GPR65 KO-AOM/DSS mice.

4. Discussion

In this study we investigated the functional role of GPR65 in the DSS-induced colitis mouse model and the AOM/DSS-induced colitis associated colorectal cancer mouse model. Our results indicate that GPR65 provides a protective role in intestinal inflammation and colitis associated colorectal cancer (CAC). The results are concordant with previous studies that demonstrate an anti-inflammatory role of GPR65 in a variety of inflammatory diseases [6, 16, 30, 31] and provide new insights into the function of GPR65 in colitis and CAC development.

GPR65 is expressed predominantly in leukocytes and can regulate the inflammatory response of immune cells [10, 12, 29, 32]. Downstream effectors of the GPR65-coupled $G\alpha_s$/cAMP demonstrate anti-inflammatory effects in a diverse set of processes [48]. $G\alpha_s$/cAMP/PKA/CREB pathway has been shown to reduce granulocyte, macrophage, and monocyte inflammatory programs [49]. Additionally, cAMP can reduce dendritic cell function in lymph nodes, T cell activation, and can increase T regulatory cell activity. These data are consistent with reports that GPR65 activation can inhibit inflammatory profiles in macrophages, microglia, neutrophils, and T cells [10, 12, 29, 32, 50]. Additionally, the anti-inflammatory role of GPR65 was demonstrated in immune-mediated murine disease models such as arthritis, lipopolysaccharide (LPS)-induced acute lung injury, myocardial infraction, ischemic stroke, and intestinal inflammation [6, 7, 16, 30, 31, 51]. However, there are also some studies suggesting GPR65 expression in eosinophils promotes inflammation through increasing eosinophil viability in an asthma mouse model [28]. Furthermore, recent studies found GPR65 is a regulator for Th17 pathogenicity and increases the severity in the experimental autoimmune encephalomyelitis (EAE) mouse model as well as increases GM-CSF production in CD4 T cells [3, 27]. Pertaining to Th17 cell pathogenicity, reports have provided evidence for both protective and pathogenic roles in the context of intestinal inflammation [52]. In addition to these *in vitro* and *in vivo* animal studies, recent genome wide association studies (GWAS) have identified single nucleotide polymorphisms (SNPs) of GPR65 associated with several human inflammatory diseases such as multiple sclerosis, asthma, heparin-induced thrombocytopenia, spondyloarthritis, and IBD [1–4, 53–55]. As previously mentioned, a recent study investigated an IBD-associated GPR65 genetic variant (I231L) within a bacteria-induced colitis mouse model and found that this GPR65 gene variant confers reduced GPR65 activity as well as impaired lysosomal function [6]. Our study focuses on the functional role of GPR65 in the regulation of inflammation and inflammation-associated carcinogenesis in a chemically induced chronic colitis mouse model which further provides evidence that GPR65 functions to inhibit inflammation in colitis. We demonstrated that GPR65 is expressed in infiltrated leukocytes within the colon of inflamed intestinal tissues using GFP as a surrogate marker in GPR65 KO mice. There

is a discernible increase in GFP positive leukocytes in the DSS treated mouse colon tissues compared to the untreated tissues indicating GPR65 expression is increased in inflamed tissues compared to non-inflamed intestinal tissues. Consistently, GPR65 gene expression is increased in human colitis and Crohn's intestinal lesions compared to non-inflamed intestinal tissues. It is likely the increased expression of GPR65 in IBD intestinal samples is partly due to the increase of infiltrated leukocytes, which have high endogenous GPR65 expression.

We also found that pathological fibrosis was increased in GPR65 KO-DSS mice compared to WT-DSS mice. Fibrosis is a serious consequence of recurrent intestinal inflammation and can lead to complications such as intestinal strictures and obstruction [42, 56, 57]. Collagen can be produced by several cellular constituents within the intestinal tissues. Some such cells include fibroblasts, sub-epithelial myofibroblasts, smooth muscle cells, and pericytes. Additionally, fibroblasts, smooth muscle cells, fibrocytes, endothelial cells, pericytes can undergo epithelial/endothelial- mesenchymal transition into myofibroblasts for wound healing functions [42, 56, 57]. Myofibroblasts are described as a major contributor of pathological extracellular matrix deposition within the inflamed intestine [42, 56, 57]. We observed GPR65 KO mice had more SMA^+ myofibroblasts than WT mice, supporting the observed increased fibrotic deposition in the DSS-treated GPR65 KO colon. It remains to be determined how GPR65 regulates fibrosis in the chronic colitis model. Interestingly, however, a recent study demonstrates that GPR65 regulates macrophage CCL20 expression, γδT cell infiltration, and fibrosis in a myocardial infarction mouse model [31]. Possibly, the increase of fibrosis is secondary to the aggravated inflammation in the DSS-treated GPR65 KO colon.

IBD patients have a higher risk of developing colorectal cancer than the general population. The cumulative incidence of colorectal cancer is 2.5–8.0% and 7.5–18.0% in IBD patients with 20 and 30 years of disease duration, respectively [43]. It has been well demonstrated that the inflamed intestinal microenvironment is a driving force for colon epithelial transformation [44]. In the inflamed milieu, inflammatory cells generate reactive oxygen species (ROS), cytokines, chemokines, and pro-angiogenic factors that induce gene mutations, promote cell proliferation and survival, and stimulate angiogenesis. Chronic intestinal inflammation drives tumor initiation and progression in colitis-associated colorectal cancer (CAC) development, referred to as the "inflammation-dysplasia-carcinoma" pathway. To further build upon our results showing GPR65 dampens intestinal inflammation, we utilized the AOM/DSS mouse model to assess the role of GPR65 in CAC development [38]. We observed the DSS insult induced elevated disease activity scores in the GPR65 KO mice when compared to WT mice in the AOM/DSS-induced CAC mouse model. Several macroscopic and microscopic disease indicators were aggravated in the GPR65 KO mice when compared to the WT in the AOM/DSS-induced CAC model. Consistent with heightened intestinal inflammation scores, colonic polyp and tumor formation was elevated in the AOM/DSS-treated GPR65 KO mice when compared to WT. Chronic, unresolved intestinal inflammation driven by leukocyte infiltration in the colon tissues can drive dysplasia from preneoplastic lesions [58]. We observed increased leukocyte infiltration in GPR65 KO AOM/DSS mice when compared to WT. Our results demonstrate that the loss of GPR65 expression in AOM/DSS mice elevates

leukocyte infiltration in the colon and suggests activation of GPR65 can suppress intestinal inflammation and colitis associated colorectal cancer development.

The development of CAC in IBD patients depends on the duration and severity of intestinal inflammation [43–45]. This makes surveillance colonoscopy as a preventative measure crucial for IBD patients to detect dysplastic lesions. Our study provides support for an anti-inflammatory role of GPR65 in colitis and suggests GPR65 could be a potential target for therapeutic intervention for IBD and CAC prevention. Currently, IBD treatment options are limited and predominantly consist of aminosalicylates (5-ASA), steroids, anti-TNFα monoclonal antibodies, and anti-integrin monoclonal antibodies [59]. The efficacy of these anti-inflammatory treatments against CAC development in IBD patients are inconclusive [60, 61]. This warrants the development of more effective approaches for IBD treatment and CAC prevention. The GPR65 agonist BTB09089 has been developed and recently investigated for anti-inflammatory properties. BTB09089 was shown to activate GPR65 *in vitro* but provided weak activity *in vivo* according to a previous study [29]. Another study has shown *in vivo* efficacy of BTB09089 using an ischemic stroke murine disease model [51]. Further studies must be done to develop highly efficacious GPR65 modulators, such as positive allosteric modulators, for potential use in IBD treatment and CAC prevention.

Supplementary Material

Refer to Web version on PubMed Central for supplementary material.

Acknowledgements

We would like to thank Luke Ashley, Nancy Leffler, Elizabeth Krewson, Lixue Dong, Calvin Justus, Joani Oswald, and Shayan Nik Akhtar for their excellent technical assistance. Additionally, we thank Dr. Owen Witte for providing the GPR65 KO mice.

Funding

This work was supported by research grants from the National Institutes of Health (1R15DK109484-01, to L.V.Y.), Brody Brothers Endowment Fund (#213817, to L.V.Y., H.H., and K.L), and Vidant Cancer Research and Education Fund (to L.V.Y).

References

[1]. Hussman JP, Beecham AH, Schmidt M, Martin ER, McCauley JL, Vance JM, Haines JL, Pericak-Vance MA, GWAS analysis implicates NF-kappaB-mediated induction of inflammatory T cells in multiple sclerosis, Genes Immun 17 (2016) 305–312. [PubMed: 27278126]

[2]. Hardin M, Cho M, McDonald ML, Beaty T, Ramsdell J, Bhatt S, van Beek EJ, Make BJ, Crapo JD, Silverman EK, Hersh CP, The clinical and genetic features of COPD-asthma overlap syndrome, Eur Respir J (2014).

[3]. Al-Mossawi MH, Chen L, Fang H, Ridley A, de Wit J, Yager N, Hammitzsch A, Pulyakhina I, Fairfax BP, Simone D, Yi Y, Bandyopadhyay S, Doig K, Gundle R, Kendrick B, Powrie F, Knight JC, Bowness P, Unique transcriptome signatures and GM-CSF expression in lymphocytes from patients with spondyloarthritis, Nat Commun 8 (2017) 1510. [PubMed: 29142230]

[4]. Jostins L, Ripke S, Weersma RK, Duerr RH, McGovern DP, Hui KY, Lee JC, Schumm LP, Sharma Y, Anderson CA, Essers J, Mitrovic M, Ning K, Cleynen I, Theatre E, Spain SL, Raychaudhuri S, Goyette P, Wei Z, Abraham C, Achkar JP, Ahmad T, Amininejad L, Ananthakrishnan AN, Andersen V, Andrews JM, Baidoo L, Balschun T, Bampton PA, Bitton A, Boucher G, Brand S, Buning C, Cohain A, Cichon S, D'Amato M, De Jong D, Devaney KL, Dubinsky M, Edwards C,

Ellinghaus D, Ferguson LR, Franchimont D, Fransen K, Gearry R, Georges M, Gieger C, Glas J, Haritunians T, Hart A, Hawkey C, Hedl M, Hu X, Karlsen TH, Kupcinskas L, Kugathasan S, Latiano A, Laukens D, Lawrance IC, Lees CW, Louis E, Mahy G, Mansfield J, Morgan AR, Mowat C, Newman W, Palmieri O, Ponsioen CY, Potocnik U, Prescott NJ, Regueiro M, Rotter JI, Russell RK, Sanderson JD, Sans M, Satsangi J, Schreiber S, Simms LA, Sventoraityte J, Targan SR, Taylor KD, Tremelling M, Verspaget HW, De Vos M, Wijmenga C, Wilson DC, Winkelmann J, Xavier RJ, Zeissig S, Zhang B, Zhang CK, Zhao H, Silverberg MS, Annese V, Hakonarson H, Brant SR, Radford-Smith G, Mathew CG, Rioux JD, Schadt EE, Daly MJ, Franke A, Parkes M, Vermeire S, Barrett JC, Cho JH, Host-microbe interactions have shaped the genetic architecture of inflammatory bowel disease, Nature 491 (2012) 119–124. [PubMed: 23128233]

[5]. Lahue KG, Lara MK, Linton AA, Lavoie B, Fang Q, McGill MM, Crothers JW, Teuscher C, Mawe GM, Tyler AL, Mahoney JM, Krementsov DN, Identification of novel loci controlling inflammatory bowel disease susceptibility utilizing the genetic diversity of wild-derived mice, Genes and immunity 21 (2020) 311–325. [PubMed: 32848229]

[6]. Lassen KG, McKenzie CI, Mari M, Murano T, Begun J, Baxt LA, Goel G, Villablanca EJ, Kuo SY, Huang H, Macia L, Bhan AK, Batten M, Daly MJ, Reggiori F, Mackay CR, Xavier RJ, Genetic Coding Variant in GPR65 Alters Lysosomal pH and Links Lysosomal Dysfunction with Colitis Risk, Immunity (2016).

[7]. Tcymbarevich I, Richards SM, Russo G, Kühn-Georgijevic J, Cosin-Roger J, Baebler K, Lang S, Bengs S, Atrott K, Bettoni C, Gruber S, Frey-Wagner I, Scharl M, Misselwitz B, Wagner CA, Seuwen K, Rogler G, Ruiz PA, Spalinger M, de Vallière C, Lack of the pH-sensing Receptor TDAG8 [GPR65] in Macrophages Plays a Detrimental Role in Murine Models of Inflammatory Bowel Disease, Journal of Crohn's & colitis 13 (2019) 245–258.

[8]. Choi JW, Lee SY, Choi Y, Identification of a putative G protein-coupled receptor induced during activation-induced apoptosis of T cells, Cell Immunol 168 (1996) 78–84. [PubMed: 8599842]

[9]. Kyaw H, Zeng Z, Su K, Fan P, Shell BK, Carter KC, Li Y, Cloning, characterization, and mapping of human homolog of mouse T-cell death-associated gene, DNA Cell Biol 17 (1998) 493–500. [PubMed: 9655242]

[10]. He XD, Tobo M, Mogi C, Nakakura T, Komachi M, Murata N, Takano M, Tomura H, Sato K, Okajima F, Involvement of proton-sensing receptor TDAG8 in the anti-inflammatory actions of dexamethasone in peritoneal macrophages, Biochem Biophys Res Commun 415 (2011) 627–631. [PubMed: 22074830]

[11]. Ishii S, Kihara Y, Shimizu T, Identification of T cell death-associated gene 8 (TDAG8) as a novel acid sensing G-protein-coupled receptor, J Biol Chem 280 (2005) 9083–9087. [PubMed: 15618224]

[12]. Jin Y, Sato K, Tobo A, Mogi C, Tobo M, Murata N, Ishii S, Im DS, Okajima F, Inhibition of interleukin-1beta production by extracellular acidification through the TDAG8/cAMP pathway in mouse microglia, J Neurochem 129 (2014) 683–695. [PubMed: 24447140]

[13]. Justus CR, Dong L, Yang LV, Acidic tumor microenvironment and pH-sensing G protein-coupled receptors, Front Physiol 4 (2013) 354. [PubMed: 24367336]

[14]. Justus CR, Sanderlin EJ, Dong L, Sun T, Chi JT, Lertpiriyapong K, Yang LV, Contextual tumor suppressor function of T cell death-associated gene 8 (TDAG8) in hematological malignancies, J Transl Med 15 (2017) 204. [PubMed: 29017562]

[15]. Li Z, Dong L, Dean E, Yang LV, Acidosis decreases c-Myc oncogene expression in human lymphoma cells: a role for the proton-sensing G protein-coupled receptor TDAG8, Int J Mol Sci 14 (2013) 20236–20255. [PubMed: 24152439]

[16]. Onozawa Y, Komai T, Oda T, Activation of T cell death-associated gene 8 attenuates inflammation by negatively regulating the function of inflammatory cells, Eur J Pharmacol 654 (2011) 315–319. [PubMed: 21238451]

[17]. Sanderlin EJ, Justus CR, Krewson EA, Yang LV, Emerging roles for the pH-sensing G protein-coupled receptors in response to acidotic stress, Cell Health Cytoskelet 7 (2015) 99–109.

[18]. Wang JQ, Kon J, Mogi C, Tobo M, Damirin A, Sato K, Komachi M, Malchinkhuu E, Murata N, Kimura T, Kuwabara A, Wakamatsu K, Koizumi H, Uede T, Tsujimoto G, Kurose H, Sato T, Harada A, Misawa N, Tomura H, Okajima F, TDAG8 is a proton-sensing and psychosine-

sensitive G-protein-coupled receptor, The Journal of biological chemistry 279 (2004) 45626–45633. [PubMed: 15326175]

[19]. Lardner A, The effects of extracellular pH on immune function, Journal of leukocyte biology 69 (2001) 522–530. [PubMed: 11310837]

[20]. Fallingborg J, Christensen LA, Jacobsen BA, Rasmussen SN, Very low intraluminal colonic pH in patients with active ulcerative colitis, Dig Dis Sci 38 (1993) 1989–1993. [PubMed: 8223071]

[21]. Nugent SG, Kumar D, Rampton DS, Evans DF, Intestinal luminal pH in inflammatory bowel disease: possible determinants and implications for therapy with aminosalicylates and other drugs, Gut 48 (2001) 571–577. [PubMed: 11247905]

[22]. Chen A, Dong L, Leffler NR, Asch AS, Witte ON, Yang LV, Activation of GPR4 by acidosis increases endothelial cell adhesion through the cAMP/Epac pathway, PLoS One 6 (2011) e27586. [PubMed: 22110680]

[23]. Dong L, Krewson EA, Yang LV, Acidosis Activates Endoplasmic Reticulum Stress Pathways through GPR4 in Human Vascular Endothelial Cells, Int J Mol Sci 18 (2017) 278.

[24]. Dong L, Li Z, Leffler NR, Asch AS, Chi JT, Yang LV, Acidosis Activation of the Proton-Sensing GPR4 Receptor Stimulates Vascular Endothelial Cell Inflammatory Responses Revealed by Transcriptome Analysis, PLoS One 8 (2013) e61991. [PubMed: 23613998]

[25]. Sanderlin EJ, Leffler NR, Lertpiriyapong K, Cai Q, Hong H, Bakthavatchalu V, Fox JG, Oswald JZ, Justus CR, Krewson EA, O'Rourke D, Yang LV, GPR4 deficiency alleviates intestinal inflammation in a mouse model of acute experimental colitis, Biochim Biophys Acta 1863 (2017) 569–584.

[26]. Krewson EA, Sanderlin EJ, Marie MA, Akhtar SN, Velcicky J, Loetscher P, Yang LV, The Proton-Sensing GPR4 Receptor Regulates Paracellular Gap Formation and Permeability of Vascular Endothelial Cells, iScience 23 (2020) 100848. [PubMed: 32058960]

[27]. Gaublomme JT, Yosef N, Lee Y, Gertner RS, Yang LV, Wu C, Pandolfi PP, Mak T, Satija R, Shalek AK, Kuchroo VK, Park H, Regev A, Single-Cell Genomics Unveils Critical Regulators of Th17 Cell Pathogenicity, Cell 163 (2015) 1400–1412. [PubMed: 26607794]

[28]. Kottyan LC, Collier AR, Cao KH, Niese KA, Hedgebeth M, Radu CG, Witte ON, Khurana Hershey GK, Rothenberg ME, Zimmermann N, Eosinophil viability is increased by acidic pH in a cAMP- and GPR65-dependent manner, Blood 114 (2009) 2774–2782. [PubMed: 19641187]

[29]. Onozawa Y, Fujita Y, Kuwabara H, Nagasaki M, Komai T, Oda T, Activation of T cell death-associated gene 8 regulates the cytokine production of T cells and macrophages in vitro, Eur J Pharmacol 683 (2012) 325–331. [PubMed: 22445881]

[30]. Tsurumaki H, Mogi C, Aoki-Saito H, Tobo M, Kamide Y, Yatomi M, Sato K, Dobashi K, Ishizuka T, Hisada T, Yamada M, Okajima F, Protective Role of Proton-Sensing TDAG8 in Lipopolysaccharide-Induced Acute Lung Injury, Int J Mol Sci 16 (2015) 28931–28942. [PubMed: 26690120]

[31]. Nagasaka A, Mogi C, Ono H, Nishi T, Horii Y, Ohba Y, Sato K, Nakaya M, Okajima F, Kurose H, The proton-sensing G protein-coupled receptor T-cell death-associated gene 8 (TDAG8) shows cardioprotective effects against myocardial infarction, Sci Rep 7 (2017) 7812. [PubMed: 28798316]

[32]. Mogi C, Tobo M, Tomura H, Murata N, He XD, Sato K, Kimura T, Ishizuka T, Sasaki T, Sato T, Kihara Y, Ishii S, Harada A, Okajima F, Involvement of proton-sensing TDAG8 in extracellular acidification-induced inhibition of proinflammatory cytokine production in peritoneal macrophages, J Immunol 182 (2009) 3243–3251. [PubMed: 19234222]

[33]. Xavier RJ, Podolsky DK, Unravelling the pathogenesis of inflammatory bowel disease, Nature 448 (2007) 427–434. [PubMed: 17653185]

[34]. Philip M, Rowley DA, Schreiber H, Inflammation as a tumor promoter in cancer induction, Seminars in cancer biology 14 (2004) 433–439. [PubMed: 15489136]

[35]. Jess T, Rungoe C, Peyrin-Biroulet L, Risk of colorectal cancer in patients with ulcerative colitis: a meta-analysis of population-based cohort studies, Clinical gastroenterology and hepatology : the official clinical practice journal of the American Gastroenterological Association 10 (2012) 639–645. [PubMed: 22289873]

[36]. Radu CG, Cheng D, Nijagal A, Riedinger M, McLaughlin J, Yang LV, Johnson J, Witte ON, Normal immune development and glucocorticoid-induced thymocyte apoptosis in mice deficient for the T-cell death-associated gene 8 receptor, Mol Cell Biol 26 (2006) 668–677. [PubMed: 16382156]

[37]. Chassaing B, Aitken JD, Malleshappa M, Vijay-Kumar M, Dextran sulfate sodium (DSS)-induced colitis in mice, Curr Protoc Immunol 104 (2014) Unit 15 25.

[38]. Thaker AI, Shaker A, Rao MS, Ciorba MA, Modeling colitis-associated cancer with azoxymethane (AOM) and dextran sulfate sodium (DSS), Journal of visualized experiments : JoVE (2012) 4100. [PubMed: 22990604]

[39]. Krause P, Zahner SP, Kim G, Shaikh RB, Steinberg MW, Kronenberg M, The Tumor Necrosis Factor Family Member TNFSF14 (LIGHT) Is Required for Resolution of Intestinal Inflammation in Mice, Gastroenterology 146 (2014) 1752–1762.e1754. [PubMed: 24560868]

[40]. Sanderlin EJ, Marie M, Velcicky J, Loetscher P, Yang LV, Pharmacological inhibition of GPR4 remediates intestinal inflammation in a mouse colitis model, European Journal of Pharmacology 852 (2019) 218–230. [PubMed: 30930250]

[41]. Ding S, Walton KL, Blue RE, McNaughton K, Magness ST, Lund PK, Mucosal healing and fibrosis after acute or chronic inflammation in wild type FVB-N mice and C57BL6 procollagen alpha1(I)-promoter-GFP reporter mice, PLoS One 7 (2012) e42568. [PubMed: 22880035]

[42]. Lund PK, Zuniga CC, Intestinal fibrosis in human and experimental inflammatory bowel disease, Curr Opin Gastroenterol 17 (2001) 318–323. [PubMed: 17031177]

[43]. Stidham RW, Higgins PDR, Colorectal Cancer in Inflammatory Bowel Disease, Clin Colon Rectal Surg 31 (2018) 168–178. [PubMed: 29720903]

[44]. Ullman TA, Itzkowitz SH, Intestinal inflammation and cancer, Gastroenterology 140 (2011) 1807–1816. [PubMed: 21530747]

[45]. Eaden JA, Abrams KR, Mayberry JF, The risk of colorectal cancer in ulcerative colitis: a meta-analysis, Gut 48 (2001) 526–535. [PubMed: 11247898]

[46]. Robertis M, Massi E, Poeta M, Carotti S, Morini S, Cecchetelli L, Signori E, Fazio V, The AOM/DSS murine model for the study of colon carcinogenesis: From pathways to diagnosis and therapy studies, J Carcinog 10 (2011) 9–9. [PubMed: 21483655]

[47]. Zhang Y, Pu W, Bousquenaud M, Cattin S, Zaric J, Sun LK, Rüegg C, Emodin Inhibits Inflammation, Carcinogenesis, and Cancer Progression in the AOM/DSS Model of Colitis-Associated Intestinal Tumorigenesis, Front Oncol 10 (2020) 564674. [PubMed: 33489875]

[48]. Mosenden R, Tasken K, Cyclic AMP-mediated immune regulation--overview of mechanisms of action in T cells, Cell Signal 23 (2011) 1009–1016. [PubMed: 21130867]

[49]. Raker VK, Becker C, Steinbrink K, The cAMP Pathway as Therapeutic Target in Autoimmune and Inflammatory Diseases, Front Immunol 7 (2016) 123. [PubMed: 27065076]

[50]. Murata N, Mogi C, Tobo M, Nakakura T, Sato K, Tomura H, Okajima F, Inhibition of superoxide anion production by extracellular acidification in neutrophils, Cell Immunol 259 (2009) 21–26. [PubMed: 19539899]

[51]. Ma XD, Hang LH, Shao DH, Shu WW, Hu XL, Luo H, TDAG8 activation attenuates cerebral ischaemia-reperfusion injury via Akt signalling in rats, Exp Neurol 293 (2017) 115–123. [PubMed: 28365474]

[52]. Galvez J, Role of Th17 Cells in the Pathogenesis of Human IBD, ISRN Inflamm 2014 (2014) 928461. [PubMed: 25101191]

[53]. Karnes JH, Cronin RM, Rollin J, Teumer A, Pouplard C, Shaffer CM, Blanquicett C, Bowton EA, Cowan JD, Mosley JD, Van Driest SL, Weeke PE, Wells QS, Bakchoul T, Denny JC, Greinacher A, Gruel Y, Roden DM, A genome-wide association study of heparin-induced thrombocytopenia using an electronic medical record, Thromb Haemost 113 (2015) 772–781. [PubMed: 25503805]

[54]. Tcymbarevich IV, Eloranta JJ, Rossel JB, Obialo N, Spalinger M, Cosin-Roger J, Lang S, Kullak-Ublick GA, Wagner CA, Scharl M, Seuwen K, Ruiz PA, Rogler G, de Vallière C, Misselwitz B, The impact of the rs8005161 polymorphism on G protein-coupled receptor GPR65 (TDAG8) pH-associated activation in intestinal inflammation, BMC gastroenterology 19 (2019) 2. [PubMed: 30616622]

[55]. Yuan Y, Ma Y, Zhang X, Han R, Hu X, Yang J, Wang M, Guan SY, Pan G, Xu SQ, Jiang S, Pan F, Genetic polymorphisms of G protein-coupled receptor 65 gene are associated with ankylosing spondylitis in a Chinese Han population: A case-control study, Human immunology 80 (2019) 146–150. [PubMed: 30529363]

[56]. Latella G, Di Gregorio J, Flati V, Rieder F, Lawrance IC, Mechanisms of initiation and progression of intestinal fibrosis in IBD, Scand J Gastroenterol 50 (2015) 53–65. [PubMed: 25523556]

[57]. Rieder F, Fiocchi C, Intestinal fibrosis in inflammatory bowel disease - Current knowledge and future perspectives, J Crohns Colitis 2 (2008) 279–290. [PubMed: 21172225]

[58]. Risques RA, Lai LA, Himmetoglu C, Ebaee A, Li L, Feng Z, Bronner MP, Al-Lahham B, Kowdley KV, Lindor KD, Rabinovitch PS, Brentnall TA, Ulcerative colitis-associated colorectal cancer arises in a field of short telomeres, senescence, and inflammation, Cancer research 71 (2011) 1669–1679. [PubMed: 21363920]

[59]. Chandel S, Prakash A, Medhi B, Current scenario in inflammatory bowel disease: drug development prospects, Pharmacol Rep 67 (2015) 224–229. [PubMed: 25712643]

[60]. Bernstein CN, Nugent Z, Blanchard JF, 5-aminosalicylate is not chemoprophylactic for colorectal cancer in IBD: a population based study, Am J Gastroenterol 106 (2011) 731–736. [PubMed: 21407180]

[61]. Burr NE, Hull MA, Subramanian V, Does aspirin or non-aspirin non-steroidal anti-inflammatory drug use prevent colorectal cancer in inflammatory bowel disease?, World journal of gastroenterology 22 (2016) 3679–3686. [PubMed: 27053860]

Highlights

- GPR65 is highly expressed in leukocytes and overexpressed in inflamed intestines.
- GPR65 knockout exacerbates intestinal inflammation in the mouse colitis model.
- GPR65 knockout aggravates colitis-associated colorectal tumorigenesis in mice.

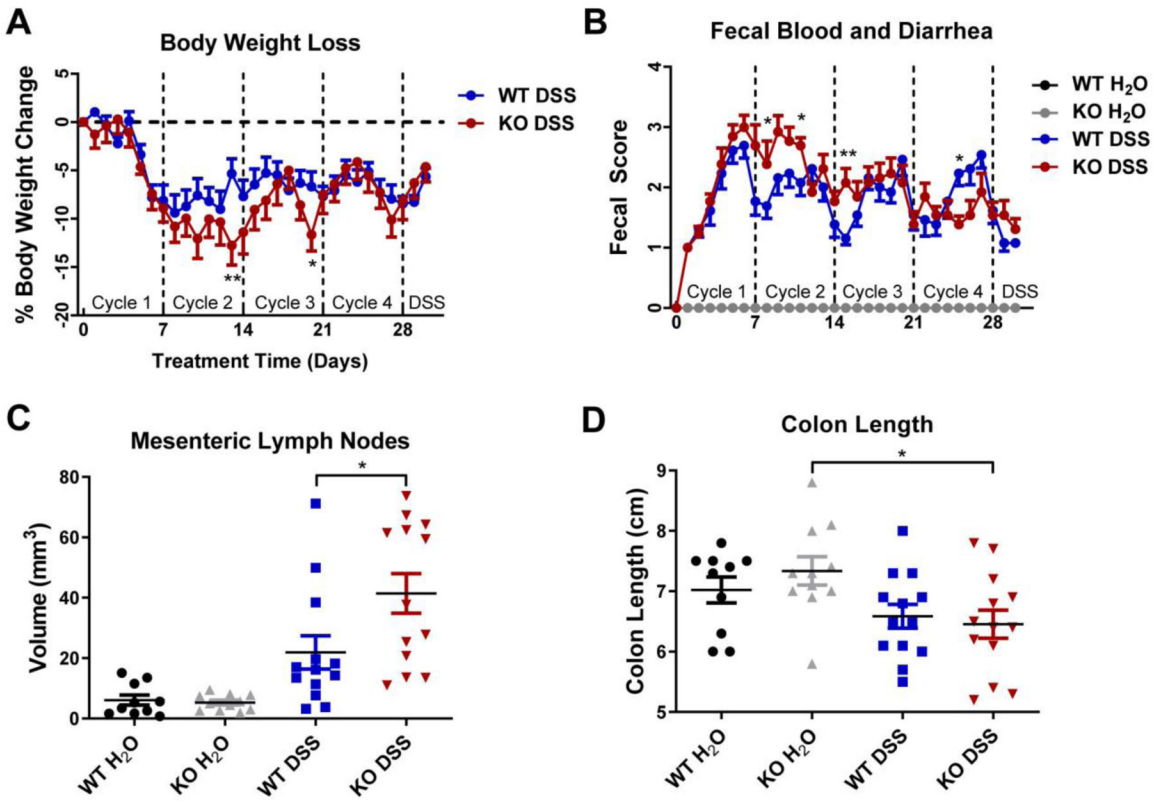

Figure 1.

Disease indicators of chronic colitis induction in wild-type (WT) and GPR65 knockout (KO) mice. The extent of DSS-induced intestinal inflammation was assessed in WT-DSS and GPR65 KO-DSS mice. WT and GPR65 KO mice given regular water served as the control. GPR65 KO-DSS mice presented elevated disease parameters compared to WT-DSS mice. Clinical phenotypes of intestinal inflammation such as (A) body weight loss normalized to control mice and (B) fecal blood and diarrhea were assessed. Macroscopic disease indicators such as (C) mesenteric lymph node expansion and (D) colon shortening were also recorded. Data are presented as the mean ± SEM and statistical significance was determined using the unpaired *t*-test between WT-DSS and GPR65 KO-DSS groups. WT control (N=10, with 5 males and 5 females), WT-DSS (N=13, with 6 males and 7 females), GPR65 KO control (N=11, with 5 males and 6 females), and GPR65 KO-DSS (N=13, with 6 males and 7 females) mice were used for experiments. (*$P < 0.05$, **$P < 0.01$).

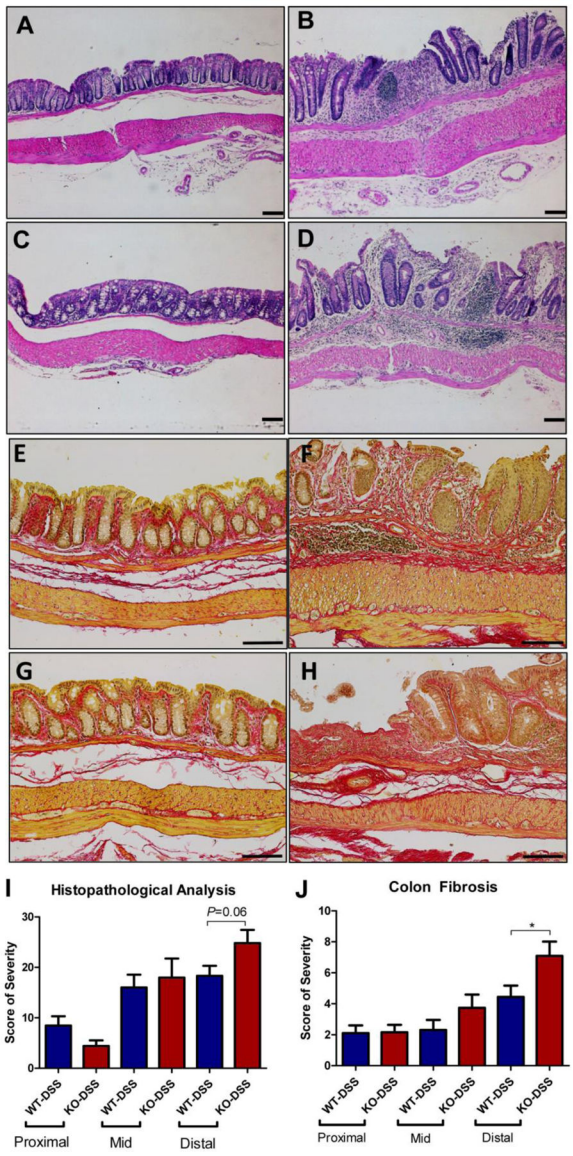

Figure 2.

Histopathological analysis of proximal, middle, and distal colon. Characteristic histopathological features of colitis were assessed to further characterize the degree of intestinal inflammation. GPR65 KO-DSS mice presented elevated disease parameters compared to WT-DSS mice. Representative H&E pictures were taken for (A) WT control, (B) WT-DSS, (C) GPR65 KO control, and (D) GPR65 KO-DSS mice. Representative pictures of Picrosirius red stained tissue sections for fibrosis assessment were taken of (E) WT control, (F) WT-DSS, (G) GPR65 KO control, and (H) GPR65 KO-DSS mice. Graphical representation of (I) total histopathological scores and (J) colonic fibrosis are presented. WT control (N=10), WT-DSS (N=13), GPR65 KO control (N=11), and GPR65 KO-DSS (N=13) mouse tissues were used for histopathological analysis. Scale bar is 100μm. Data are presented as the mean ± SEM and statistical significance was determined using the unpaired *t*-test between WT-DSS and GPR65 KO-DSS groups. (**P* < 0.05).

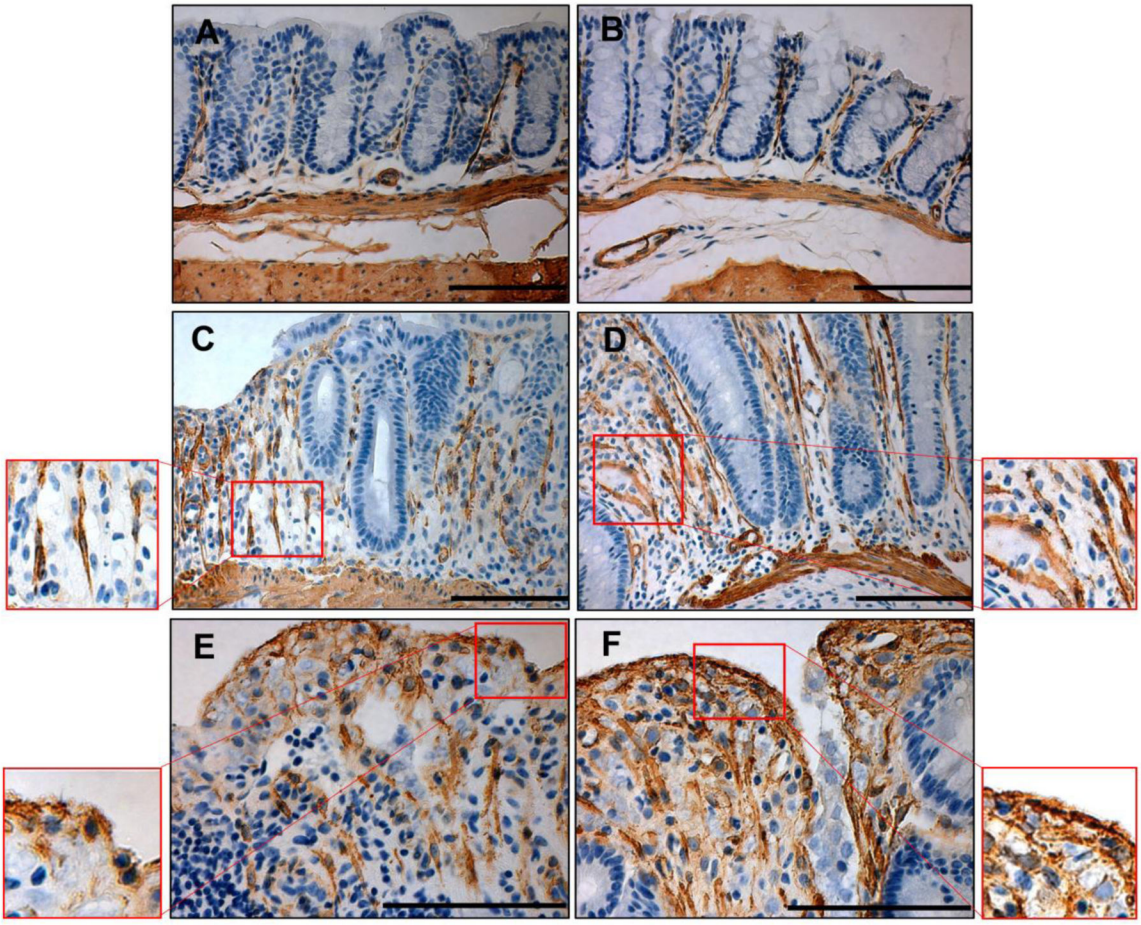

Figure 3.

Myofibroblast expansion in distal colon mucosa. SMA^{+} myofibroblasts were evaluated in distal colon as a cellular basis for increased colonic fibrosis. Representative pictures of (A) WT control, (B) GPR65 KO-control, (C,E) WT-DSS, and (D,F) GPR65 KO-DSS. Scale bar is 100μm.

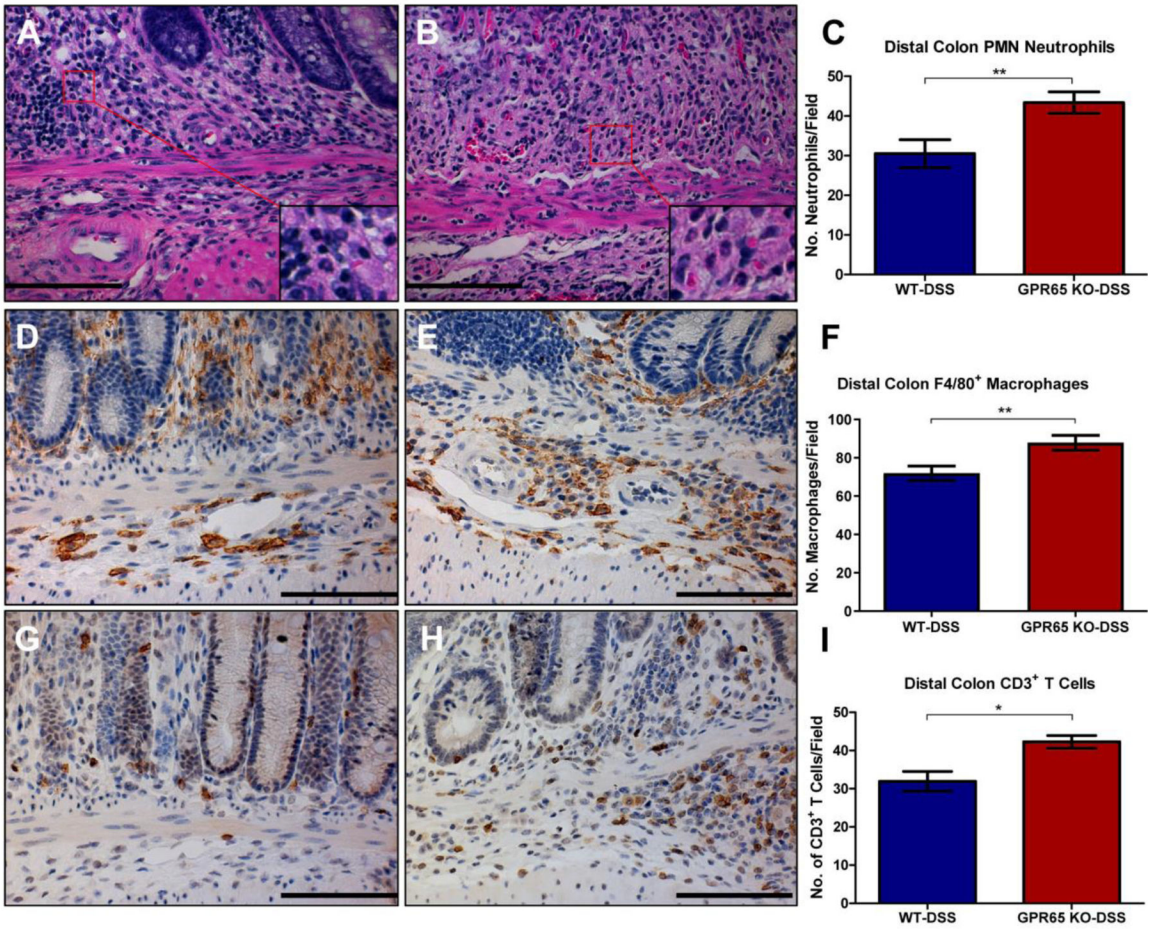

Figure 4.

Leukocyte infiltrates in distal colon. Polymorphonuclear (PMN) neutrophils, F4/80$^+$ macrophages, and CD3$^+$ T cells were counted in the distal colon. GPR65 KO-DSS mice had increased neutrophils, macrophages, and T cells in distal colon when compared to WT-DSS mice. (A) Representative pictures of WT-DSS (left) and GPR65 KO-DSS (right) mouse (A-B) neutrophils, (D-E) macrophages, and (G-H) T cells, respectively. Graphical representation of (C) neutrophils, (F) macrophages, (I) and T cells. Scale bar is 100μm. Data are presented as the mean ± SEM and statistical significance was determined using the unpaired *t*-test between WT-DSS and GPR65 KO-DSS groups. (*$P < 0.05$, **$P < 0.01$).

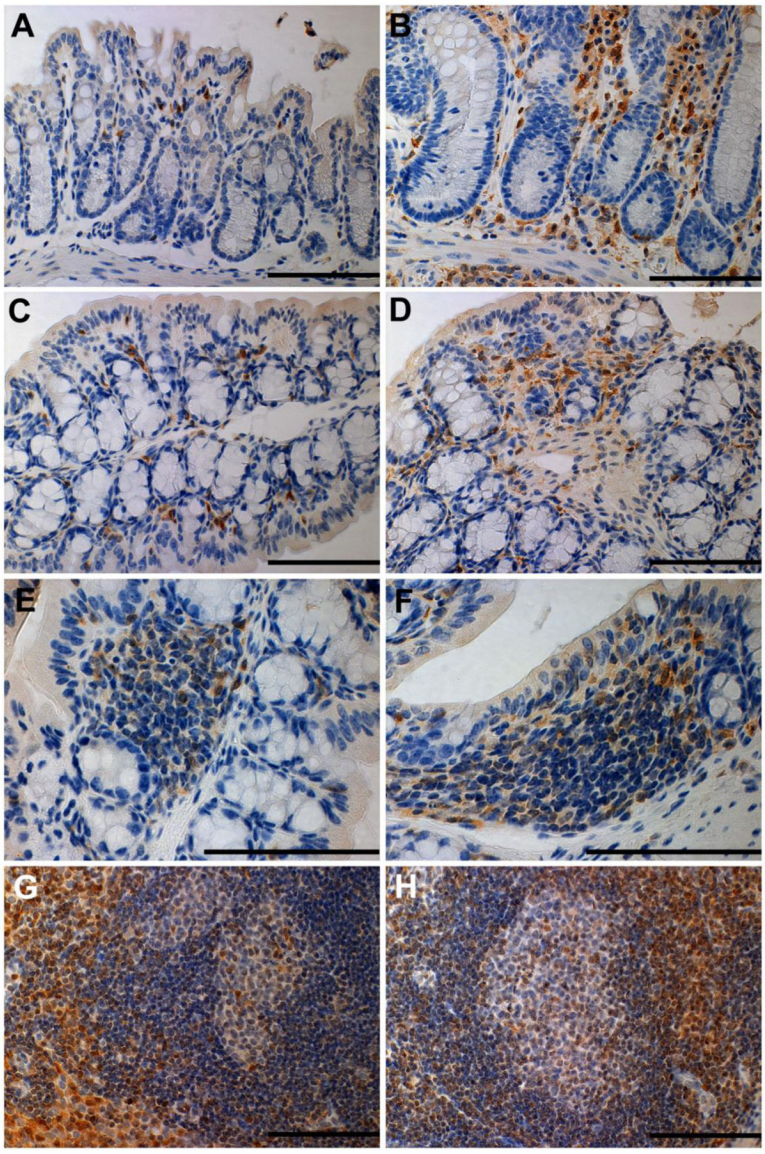

Figure 5.

GFP signal in the intestine and intestinal associated lymphoid tissues. GFP knock-in signal under the control of GPR65 promoter serves as a surrogate marker for endogenous GPR65 expression in GPR65 KO mice. GFP signal could be detected in GPR65 KO mouse (A) distal colon mucosa, (C) proximal colon transverse folds, (E) isolated lymphoid follicles (ILFs), and (G) mesenteric lymph nodes (MLNs). GFP signal could be detected in DSS-treated GPR65 KO (B) intestinal mucosa, (D) transverse folds, (F) ILFs, and (H) MLNs. Based on cellular morphology and localization, GFP signal was observed in intestinal and MLN macrophages, lymphocytes, and neutrophils. Scale bar is 100μm.

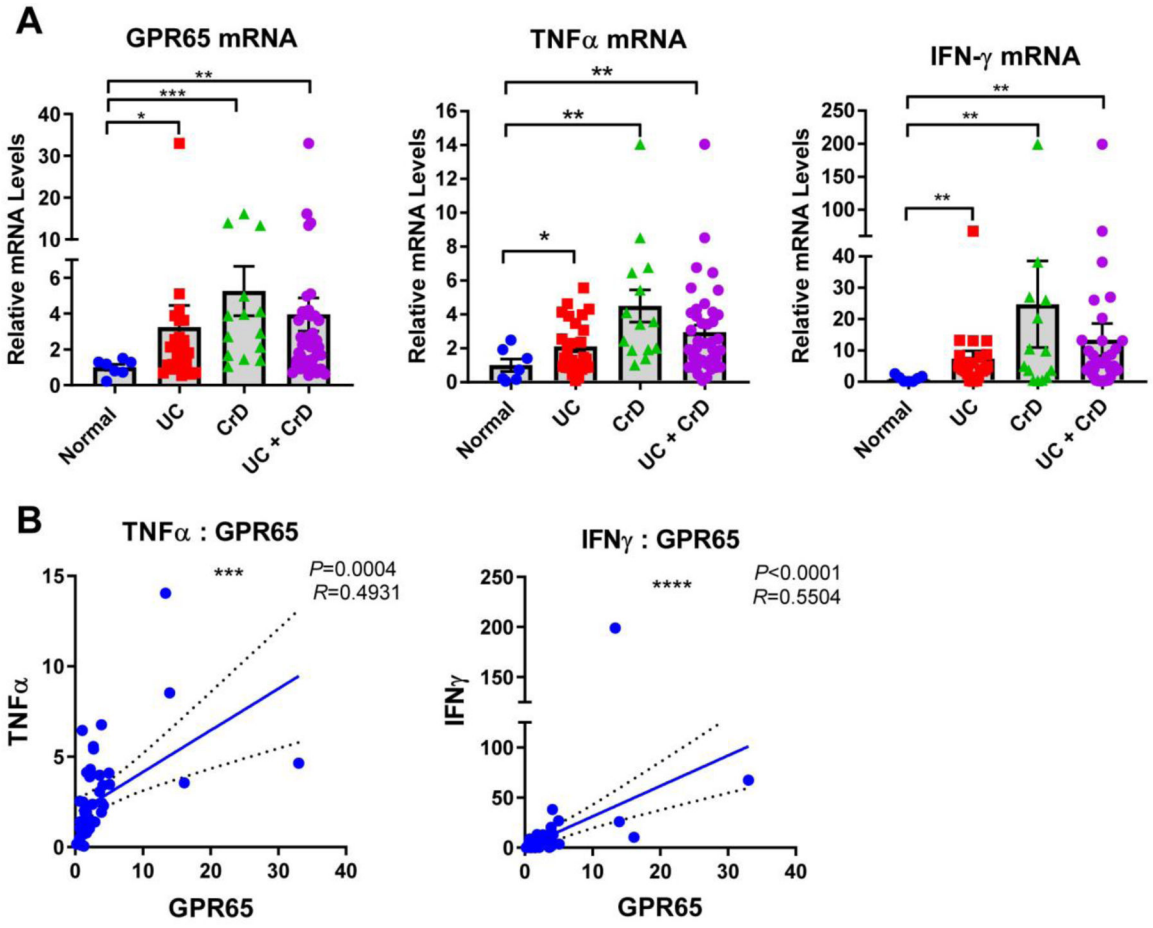

Figure 6.

GPR65 and inflammatory gene expression in human ulcerative colitis and Crohn's disease. GPR65 mRNA is increased in ulcerative colitis (UC) and Crohn's disease (CrD) compared to non-inflamed intestinal tissues and positively correlates with TNFα and IFNγ gene expression. (A) GPR65, TNFα and IFNγ mRNA levels in UC and CrD intestinal tissues. (B) Correlation of GPR65 mRNA expression with TNFα and IFNγ mRNA levels. Data are presented as the mean ± SEM and statistical significance was determined using the Mann-Whitney test between control and diseased intestinal tissues. Correlation of gene expression was determined by the linear regression analysis. (*$P < 0.05$, **$P < 0.01$, ***$P < 0.001$, ****$P < 0.0001$).

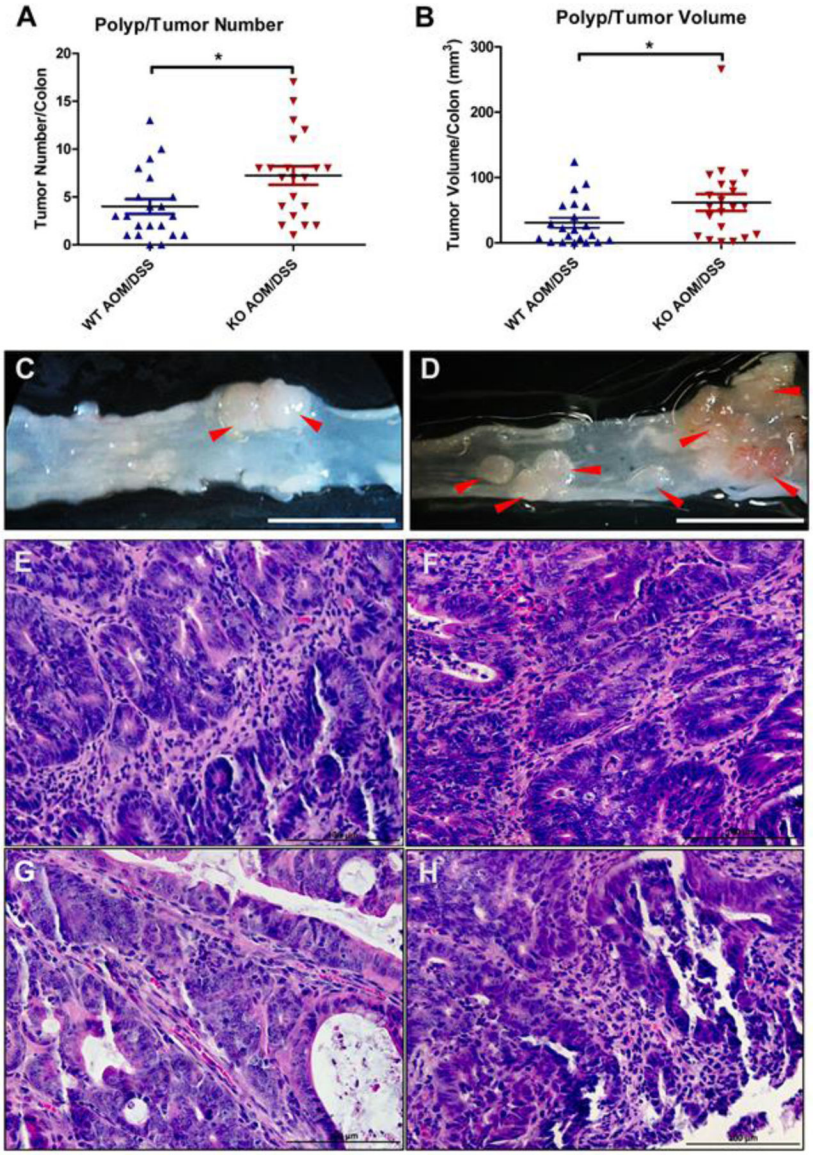

Figure 7.

Effects of GPR65 on tumorigenesis in the colitis associated colorectal cancer (CAC) mouse model. Tumor burden is increased in the colons of GPR65 KO-AOM/DSS mice (N=21, with 11 males and 10 females) compared to WT-AOM/DSS mice (N=21, with 11 males and 10 females). Red arrows indicate polyps and tumors. (A) Polyp/tumor number, (B) polyp/tumor volume, (C-D) representative pictures of distal colons bearing polyps/tumors in (C) WT and (D) GPR65 KO, and (E-H) histopathological representation of dysplasia and adenocarcinoma in (E, G) WT and (F, H) GPR65 KO AOM/DSS mouse colons. Data are presented as the mean ± SEM and statistical significance was determined using the unpaired *t*-test between WT and GPR65 KO AOM/DSS mice. (**P* <0.05).

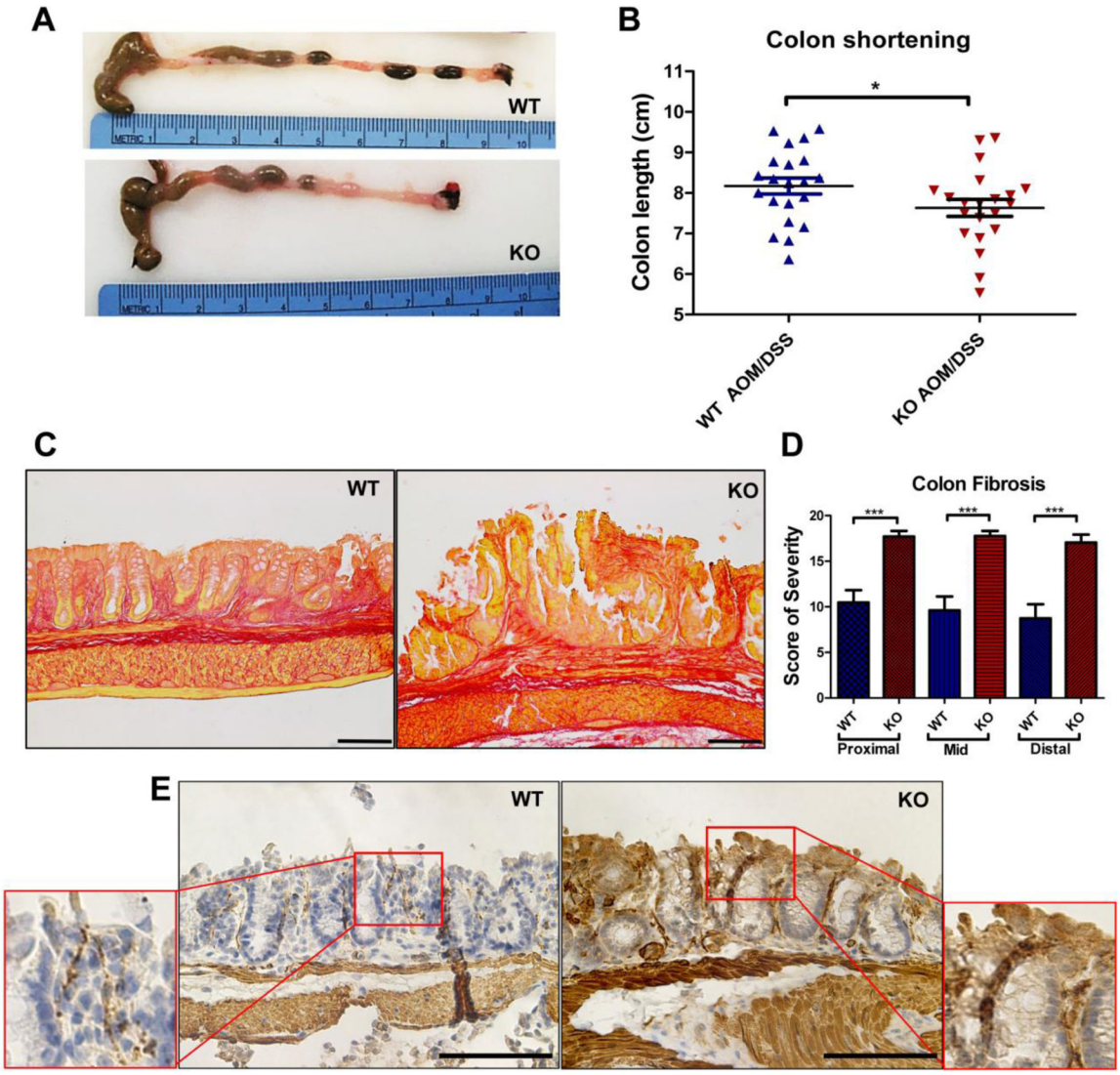

Figure 8.

Colon shortening, fibrosis, and myofibroblast expansion in AOM/DSS mice. The colons of GPR65 KO-AOM/DSS mice show reduced length, increased fibrosis, and heightened myofibroblast expansion compared to WT AOM/DSS mice. (A, B) Colon length, (C) representative images of pathological fibrosis by Picrosirius Red staining, (D) fibrosis score of severity (WT N=21 and GPR65 KO N=21), and (E) immunohistochemistry of α-SMA^{+} myofibroblasts in mouse colon tissues. Scale bar is 100μm. Data are presented as the mean ± SEM and statistical significance was determined using the unpaired *t*-test between WT AOM/DSS and GPR65 KO-AOM/DSS mice (*$P < 0.05$, ***$P < 0.001$).

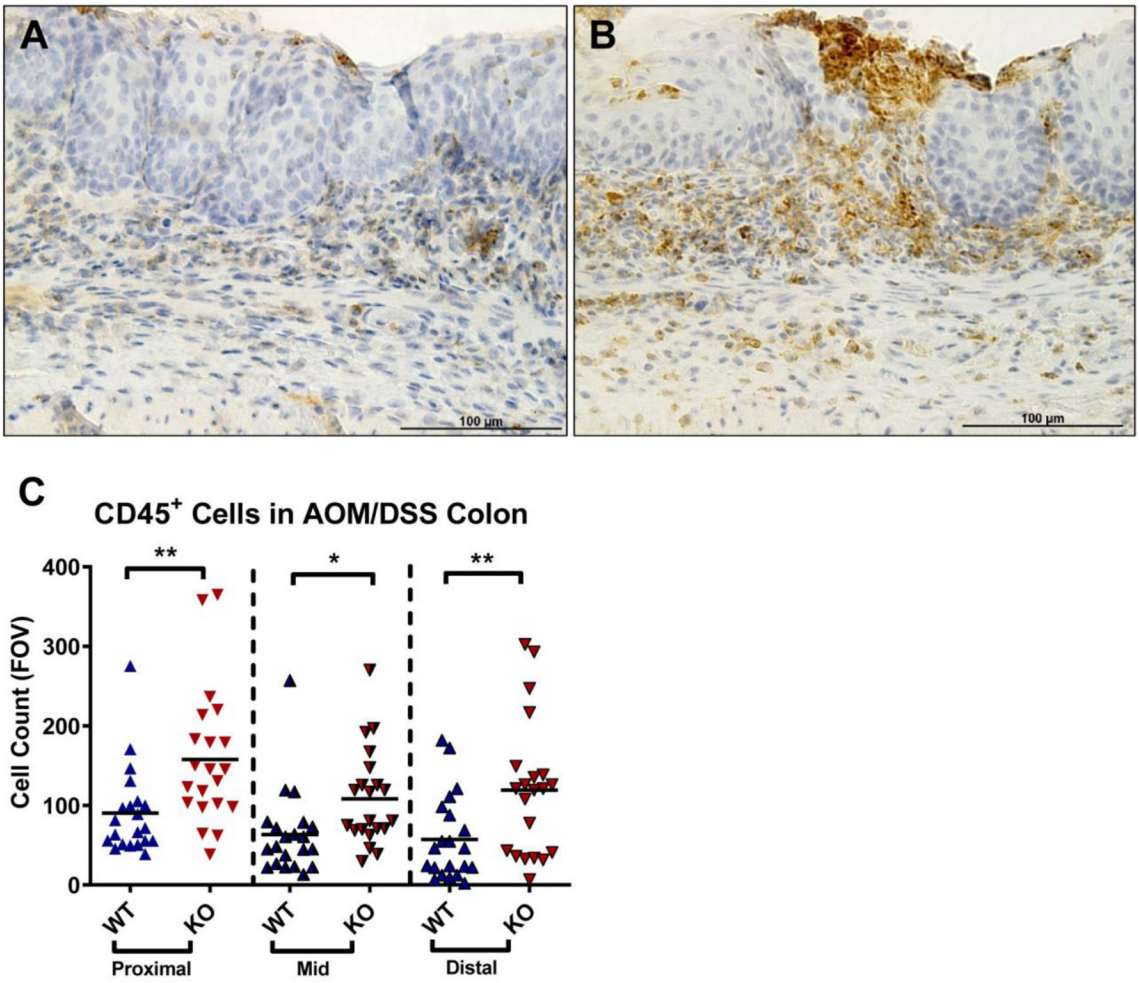

Figure 9.

Leukocyte infiltration in colons of AOM/DSS mice. Leukocyte infiltration in colon tissues is increased in GPR65 KO-AOM/DSS mice when compared to WT AOM/DSS mice. $CD45^+$ immunohistochemistry of leukocytes in (A) WT and (B) GPR65 KO AOM/DSS mouse colon sections, and (C) cell count of leukocyte infiltration in distal, middle, and proximal colon segments (WT N=21 and GPR65 KO N=21). Scale bar is 100μm. Data are presented as the mean ± SEM and statistical significance was determined using the unpaired *t*-test between WT and GPR65 KO AOM/DSS mice (*$P < 0.05$, **$P < 0.01$).